Journal of Radiotherapy in Practice

cambridge.org/jrp

Improvement of helical tomotherapy treatment plan efficiency with block techniques for left-sided post-mastectomy radiation therapy

Arisara Chirawattana[1], Imjai Chitapanarux[2] and Wannapha Nobnop[2]

[1]Faculty of Medicine, Medical Physics Program, Radiation Oncology Division, Department of Radiology, ChiangMai University, ChiangMai, Thailand and [2]Faculty of Medicine, Radiation Oncology Division, Department of Radiology, ChiangMai University, ChiangMai, Thailand

Original Article

Cite this article: Chirawattana A, Chitapanarux I, and Nobnop W. (2023) Improvement of helical tomotherapy treatment plan efficiency with block techniques for left-sided post-mastectomy radiation therapy. *Journal of Radiotherapy in Practice*. **22**(e68), 1–6. doi: 10.1017/S1460396922000450

Received: 8 July 2022
Revised: 8 November 2022
Accepted: 20 December 2022

Key words:
directional block; helical tomotherapy; integral dose; post-mastectomy; treatment time; virtual block structure

Author for correspondence:
Dr Wannapha Nobnop, Faculty of Medicine, Chiangmai University, ChiangMai, 50200, Thailand. E-mail: wannapha.n@cmu.ac.th

Abstract

Purpose: To limit the entrance dose to normal tissue and achieve the appropriate treatment time (TT) by using three different virtual structures with directional blocks for left-sided post-mastectomy radiation therapy (PMRT) with regional nodal irradiation (RNI).
Methods and materials: Ten breast cancer patients who received PMRT by helical tomotherapy were enrolled. Three virtual structures were created for each patient: Organ-based, L-shaped (LB) and C-shaped (CB). The dose to the target and organ at risk (OARs), TT, the volume which received dose 5 Gy (V_{5Gy}), integral dose (ID) and block structure contouring workload (BSCW) of the three virtual block techniques were evaluated. The performance scores were used to explore the suitable technique.
Results: The CB plans showed a significantly better V_{5Gy}, ID and contralateral breast-sparing. However, the CB plans revealed the longest TT and BSCW ($p < 0{\cdot}001$). Contrary to the LB, the LB plans showed a significantly reduced TT and BSCW and provided the balance of plan efficiency with the highest score.
Conclusion: The LB technique is considered to be the suitable technique for left-sided PMRT with RNI and provided the advantage of TT, V_{5Gy}, ID and BSCW while maintaining acceptable criteria for the target and OARs.

Introduction

For high-risk breast cancer patients, post-mastectomy radiation therapy (PMRT) has been shown to significantly reduce the probability of recurrence and improve overall survival when compared with surgery alone.[1,2] The target volume normally includes the chest wall and regional lymph nodes which is close to the lung, heart and contralateral breast.[2,3]

Helical tomotherapy (HT) is a recent treatment trend for PMRT with complex targets, especially with regional nodal irradiation (RNI), because HT demonstrated improvement of dose conformality to the target while sparing the organ at risk (OARs).[4,5] On the other hand, HT increases low-dose area and mean dose of OARs, high normal tissue complication probability for the lungs and heart, and high secondary cancer complication probability for the lungs and contralateral breast.[6] HT used without block structure has a potentially higher risk of radiation pneumonitis, cardiac disease and secondary cancer.[6] On the other hand, HT with a block structure increases the number of monitor units and treatment time (TT).[6–8] The trade-off between the TT and the plan quality should be balanced.[6] The reduction in TT may lead to improved treatment accuracy because the influence of intrafraction motion was reduced.[9] Moreover, less TT could provide the opportunity for more patients to be treated earlier and improve the treatment efficiency.

The modulation factor (MF) influences plan efficiency, freedom of the optimiser to vary beamlet intensities and TT. Using a high MF results in an increased TT. Nevertheless, reducing the MF may decrease the plan quality.[10,11]

Therefore, this study aimed to improve treatment plan efficiency for left-sided PMRT with RNI by using three different virtual structures with directional block techniques to limit the entrance beam to this structure. As a result, the difference in dosimetric parameters, plan quality, TT and the integral dose was evaluated.

Methods and Materials

Patient selection

In this study, a total of 50 treatment plans were generated from ten breast cancer patients who were treated left-sided PMRT with RNI between January 2020 and December 2020 by HT and were enrolled in this study. The patient characteristics and treatment targets are demonstrated

Table 1. Patient characteristics and treatment targets

Case	Age	Pathological staging	Target
1	51	T2N1M0	Lt. CW, SPC, IMN, AX
2	46	T2N2M0	Lt. CW, SPC, IMN, AX
3	50	T2N1M0	Lt. CW, SPC, IMN, AX
4	51	T2N1M0	Lt. CW, SPC
5	35	T2N2M0	Lt. CW, SPC, IMN, AX
6	61	T1N3M0	Lt. CW, SPC, AX
7	62	T3N1M0	Lt. CW, SPC, IMN, AX
8	75	T2N0M0	Lt. CW, SPC
9	70	T2N3M0	Lt. CW, SPC, IMN, AX
10	52	T2N3M0	Lt. CW, SPC, IMN, AX

Abbreviations: Lt. CW, left-sided chest wall; SPC, supraclavicular nodes; IMN, internal mammary nodes; AX, axillary nodes.

in Table 1. All patients had performed CT simulation in head-first supine position with both arms up on the wing board (CIVCO, USA).

Target and OARs delineation

The CT image dataset with 5 mm slice thickness was transferred to Oncentra MasterPlan 3·2 for the target and organ delineation. The clinical target volume (CTV) included the left chest wall, supraclavicular nodes, axillary nodes and internal mammary nodes. The CTV was expanded isotropically by 5 mm to create the planning target volume (PTV). The PTV was cropped 3 mm beneath the external surface. Besides, the heart, both lungs and contralateral breast were contoured as organs at risk (OARs).

Dose prescription and dose constraint

The prescription dose was 42·4 Gy in 16 fractions to 50% of the PTV ($D_{50\%}$). All plans met the criteria for cold and hot spot areas by 98% of PTV volume received more than 95% of the prescribed dose and 2% of PTV volume received less than 107% of the prescribed dose. In addition, the dose constraints for OARs are illustrated in Table 2.

HT treatment planning

The CT images dataset and structure were transferred to the tomotherapy treatment planning system version 5.1.1.6 (Accuray Incorp., Sunnyvale, CA, USA) to generate the treatment plans. HT planning parameters for all plans were 5 cm (FW), 0·287 (PF), and MF starting with 2·0.

Regarding the planning techniques, a total of ten cases, five treatment plans were generated for each case with the planning details as shown in Table 3. A total of 50 treatment plans were evaluated in terms of plan quality and treatment efficiency.

Without virtual block structures

The two treatment plans in each case were generated without additional creating virtual block structures to be the reference HT plans as follows: (1) the unblocked technique (Unblocked); no directional block was used in this technique; and (2) the organ-based directional block technique (OBDB); directional block was used to limit the primary entrance beam through the heart, both lungs and contralateral breast.[12]

Table 2. Dose constraints to PTV and OARs

Structure	Volume (%)	Dose (Gy)
PTV	50	42·4
	2	<45·4
	98	>40·3
Heart	15	10
	20	8
Heart (mean dose)		9
Ipsilateral Lung	15	31
	20	26·4
	35	17·6
	50	13
Contralateral Lung	20	13
	35	10·6
	50	9
Contralateral Breast	15	17·6
	20	9
	35	6
	50	4·4

Table 3. Five treatment planning techniques

Plan number	Plan name	Virtual block structure creation	Using directional block function
1	Unblocked	No	No
2	OBDB	No	Yes
3	OB	Yes	Yes
4	LB	Yes	Yes
5	CB	Yes	Yes

Abbreviations: OBDB, organ-based directional block technique; OB, organ-based virtual block technique; LB, L-shaped virtual block technique; CB, C-shaped virtual block technique.

With virtual block structures

The three treatment plans in each case were created in different types of virtual block structures with a directional block to limit the entrance dose to OARs (Figure 1) as follows: (1) The OB virtual block technique was created by grouping the heart and both lungs to be the virtual block structure and was subtracted from PTV with 3 cm margin expansion; (2) The L-shaped virtual block technique (LB) was created by two rectangle structures perpendicular to each other similar to 'L-' shaped on the right side out of the body contour along the length of PTV. The heart shape in the axial plane was used to define the length of the L-shaped virtual block structure; and (3) The C-shaped virtual block technique (CB) was generated by using 1 cm margin expansion from the patient's body contour and was subtracted from PTV with 9 cm margin expansion.

Plan evaluation parameters

The dose-volume histograms were calculated to evaluate the PTV and OARs. The plan evaluation was compared by following parameters[13–15]:

Table 4. Dosimetric comparisons, treatment time and contouring workload between three planning techniques

	OB	LB	CB				
Parameter	Mean ± SD	Mean ± SD	Mean ± SD	*p*-value	OB versus LB	OB versus CB	LB versus CB
PTV							
$D_{50\%}$ (Gy)	42·32 ± 0·05	42·32 ± 0·05	42·29 ± 0·06	0·111	ns	ns	ns
$V_{107\%}$ (%)	0·05 ± 0·04	0·06 ± 0·08	0·06 ± 0·05	0·697	ns	ns	ns
$V_{95\%}$ (%)	98·27 ± 0·13	98·24 ± 0·10	98·25 ± 0·10	0·725	ns	ns	ns
HI	0·082 ± 0·008	0·085 ± 0·007	0·083 ± 0·005	0·250	ns	ns	ns
CN	0·687 ± 0·040	0·698 ± 0·036	0·686 ± 0·048	0·190	ns	ns	ns
Heart							
$D_{15\%}$ (Gy)	9·86 ± 0·14	9·86 ± 0·11	9·80 ± 0·14	0·072	ns	ns	ns
$D_{20\%}$ (Gy)	7·65 ± 0·15	7·63 ± 0·12	7·59 ± 0·18	0·409	ns	ns	ns
D_{mean} (Gy)	7·04 ± 0·25	7·13 ± 0·38	7·06 ± 0·27	0·308	ns	ns	ns
Ipsilateral Lung							
$D_{15\%}$ (Gy)	30·33 ± 0·49	30·37 ± 0·42	30·24 ± 0·44	0·005	ns	ns	0·010
$D_{20\%}$ (Gy)	26·07 ± 0·36	26·09 ± 0·31	25·99 ± 0·51	0·150	ns	ns	ns
$D_{35\%}$ (Gy)	15·45 ± 1·17	15·95 ± 0·94	15·95 ± 0·91	0·068	ns	ns	ns
$D_{50\%}$ (Gy)	8·46 ± 1·48	8·84 ± 1·59	8·61 ± 0·90	0·309	ns	ns	ns
Contralateral Lung							
$D_{20\%}$ (Gy)	7·78 ± 0·53	7·93 ± 0·49	7·53 ± 0·64	0·063	ns	ns	ns
$D_{35\%}$ (Gy)	6·14 ± 0·45	6·24 ± 0·42	5·89 ± 0·53	0·058	ns	ns	ns
$D_{50\%}$ (Gy)	4·66 ± 0·62	4·68 ± 0·57	4·39 ± 0·58	0·067	ns	ns	ns
Contralateral Breast							
$D_{15\%}$ (Gy)	10·97 ± 0·44	10·77 ± 0·46	8·76 ± 2·09	0·003	ns	0·008	0·015
$D_{20\%}$ (Gy)	8·86 ± 0·07	8·80 ± 0·16	7·13 ± 1·03	<0·001	ns	<0·001	<0·001
$D_{35\%}$ (Gy)	5·60 ± 0·22	5·55 ± 0·21	5·12 ± 0·31	<0·001	ns	0·023	0·004
$D_{50\%}$ (Gy)	4·30 ± 0·07	4·26 ± 0·08	4·25 ± 0·11	0·146	ns	ns	ns
Whole body							
V_{5Gy} (%)	43·97 ± 4·50	40·83 ± 4·28	38·75 ± 3·24	<0·001	0·002	<0·001	ns
Integral dose (Gy·L)	165·24 ± 32·62	157·74 ± 29·61	152·08 ± 27·57	<0·001	<0·001	<0·001	0·035
Treatment time (seconds)	449·77 ± 69·50	449·71 ± 71·29	567·00 ± 114·99	<0·001	ns	<0·001	0·002
Contouring workload (seconds)	560·20 ± 33·85	467·00 ± 35·11	1018·00 ± 95·17	<0·001	<0·001	<0·001	<0·001

Abbreviations: OB, organ-based virtual block technique; LB, L-shaped virtual block technique; CB, C-shaped virtual block technique; HI, homogeneity index; CN, conformation number; ns, no statistically significant difference ($p > 0.05$).

Figure 1. The planning target volume (blue) and virtual block structure (yellow) for (a) organ-based; OB, (b) L-shaped; LB and (c) C-shaped; CB on the transverse view of computed tomography (CT) images.

https://doi.org/10.1017/S1460396922000450 Published online by Cambridge University Press

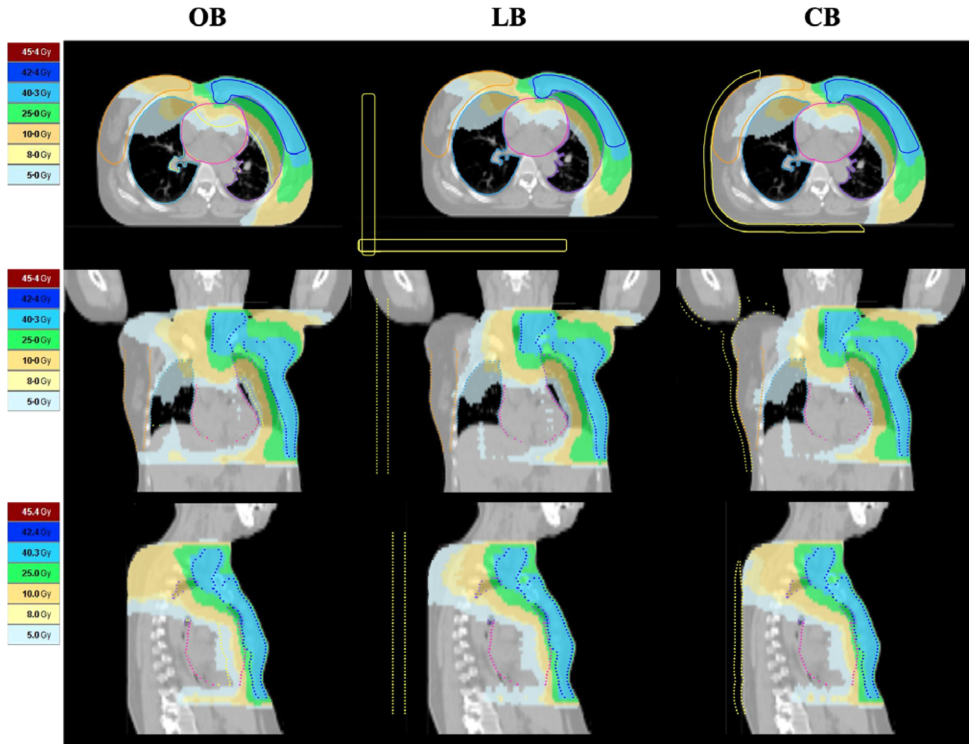

Figure 2. The dose distribution of axial, coronal and sagittal plane for three virtual block planning techniques: (a) organ-based; OB, (b) L-shaped; LB and (c) C-shaped; CB.

1. Homogeneity index for PTV was defined as follows:

$$HI = \frac{D_{2\%} - D_{98\%}}{D_{50\%}}$$

where $D_{2\%}$, $D_{50\%}$ and $D_{98\%}$ are the dose received by 2%, 50% and 98% of PTV, respectively. The HI value of 0 was represented as ideal homogeneity.

2. Conformation number for PTV was defined as follows:

$$CN = \frac{TV_{RI95\%}}{TV} \times \frac{TV_{RI95\%}}{V_{RI95\%}}$$

where TV is the target volume, $TV_{RI95\%}$ is the target volume covered by the reference isodose (95%), and $V_{RI95\%}$ is the volume of reference isodose (95%). The CN value of 1 was represented as ideal conformity.

3. Integral dose of radiation delivered to the whole patient's body was defined as follows:

$$ID\ [Gy \cdot L] = D_{mean}\ [Gy] \times V\ [L]$$

where D mean is the mean dose delivered to the whole patient's body, and V is the whole patient's body volume.

4. TT was defined as a beam on time that was associated with total monitor units of each technique; and
5. Block structure contouring workload was defined as time-consuming for delineating the additional virtual structures in the contouring process of each technique.

Statistical methods

All statistical analyses were performed by using the SPSS statistics 26. The normal distributions were investigated by Shapiro-Wilk test. Regarding the dosimetric analysis, ANOVA was used for comparison of normal distributions, while the Friedman test was used in case if the distributions were not normal. The paired sample t-test and the Wilcoxon signed-rank test were used to compare score parameters between two groups. A p-value $< 0{\cdot}05$ was considered statistically significant.

The performance score was used to explore the suitable plan by summation of the score of each parameter in each technique which was defined as '0', '1' and '2' when the p-value was $> 0{\cdot}05$, $< 0{\cdot}05$ and $< 0{\cdot}001$, respectively, and then comparing the sums with the highest one.[12]

This retrospective study recruited the CT images of the patient in the period from January 2020 to December 2020. The ethical clearance was approved by the Institutional Review Board of the Faculty of Medicine ChiangMai University (Study code: RAD-2564-08094/Research ID: 8094).

Results

Dosimetric comparisons of the PTV, OARs, V_{5Gy} and integral dose of whole body, TT and block structure contouring workload for three virtual block planning techniques are shown in Table 4. There were no statistically significant differences in dosimetric parameters of PTV, heart, both lungs except $D_{15\%}$ of ipsilateral lung and $D_{50\%}$ of the contralateral breast. All three virtual block planning techniques reached the acceptable dosimetric criteria for target and OARs. However, there were statistically significant differences with the highest V_{5Gy} ($43{\cdot}97 \pm 4{\cdot}5\%$) and integral dose ($165{\cdot}24 \pm 32{\cdot}62$ Gy·L) in the OB plans as the highest low-dose spread is displayed in Figure 2.

Another statistically significant difference was found that the LB plans provided the shortest block structure contouring workload ($467 \pm 35{\cdot}11$ seconds). Additionally, the CB plans provided the lowest $D_{15\%}$ ($8{\cdot}76 \pm 2{\cdot}09$ Gy), $D_{20\%}$ ($7{\cdot}13 \pm 1{\cdot}03$ Gy) and $D_{35\%}$ ($5{\cdot}12 \pm 0{\cdot}31$ Gy) of the contralateral breast and integral dose

https://doi.org/10.1017/S1460396922000450 Published online by Cambridge University Press

Table 5. Planned score table of three planning techniques

Parameter	OB	LB	CB
PTV			
$D_{50\%}$	0	0	0
$V_{107\%}$	0	0	0
$V_{95\%}$	0	0	0
HI	0	0	0
CN	0	0	0
Heart			
$D_{15\%}$	0	0	0
$D_{20\%}$	0	0	0
D_{mean}	0	0	0
Ipsilateral Lung			
$D_{15\%}$	0	0	1
$D_{20\%}$	0	0	0
$D_{35\%}$	0	0	0
$D_{50\%}$	0	0	0
Contralateral Lung			
$D_{20\%}$	0	0	0
$D_{35\%}$	0	0	0
$D_{50\%}$	0	0	0
Contralateral Breast			
$D_{15\%}$	0	0	2
$D_{20\%}$	0	0	4
$D_{35\%}$	0	0	2
$D_{50\%}$	0	0	0
Whole body			
V_{5Gy}	0	1	2
Integral dose	0	2	3
Treatment time	2	1	0
Contouring workload	2	4	0
Total score	4	8	14
p-value	0·151	0·256	
Score from interested parameters	4	8	5
p-value	0·252		0·571

Abbreviations: OB, organ-based virtual block technique; LB, L-shaped virtual block technique; CB, C-shaped virtual block technique.

(152·08 ± 27·57 Gy·L) and the longest TT (567 ± 114·99 seconds) and block structure contouring workload (1018 ± 95·17 seconds).

The comparisons of the performance score for three virtual block planning techniques are summarised in Table 5. The summation of the scores from all parameters in OB, LB and CB plans was 4, 8 and 14 points, respectively. Therefore, the results with the highest score demonstrated the superiority of the CB plan to spare contralateral breast and also reduce V_{5Gy} and integral dose. For clinical practice, other important factors, such as TT, should be considered. The consideration issue for HT involves balancing issues relating to a low-dose bath and TT. The LB technique was optimal because it provided acceptable dosimetric parameters, reasonable low-dose spread and a satisfactory TT. According to the summed scores, the LB plans (8 points) demonstrated the highest score when compared with OB (4 points) and CB (5 points) for TT, block structure workload and low-dose spreading as V_{5Gy} and integral dose parameters. Therefore, the results with the highest score demonstrated the superiority of the LB plan in all clinical practice parameters. However, no significant differences were found.

Discussion

The dosimetric parameters of three virtual block treatment planning techniques were evaluated using multivariate analysis to determine the optimal planning technique. The unblocked and OBDB techniques were created as the reference plans. The unblocked plans showed the advantage of TT and block structure contouring workload despite providing a very high V_{5Gy}, integral dose and dose to contralateral organs. Compared with the unblocked plans, the OBDB plans showed the advantage of contralateral lung and contralateral breast-sparing, V_{5Gy} and integral dose while providing a very long TT. Similar results have been reported by Tang et al.[6] for PMRT with SIB by HT. They revealed that the complete block function significantly reduced the dose to the lungs and heart but provided a significantly higher amount of MU and longer TT.

The mean V_{5Gy} were 43·97 ± 4·5% (OB), 40·83 ± 4·28% (LB), and 38·75 ± 3·24% (CB). Moreover, the integral dose were 165·24 ± 32·62 Gy·L, 157·74 ± 29·61 Gy·L, and 152·08 ± 27·57 Gy·L for the OB, LB and CB plans, respectively.

Another consideration point for HT with block structure is the TT, which was 7·5 ± 1·2 minutes (range 6·3–10·4 minutes), 7·5 ± 1·2 minutes (range 6·1–10·3 minutes) and 9·5 ± 1·9 minutes (range 7·5–13·7 minutes) in OB, LB and CB plans, respectively. The LB and OB plans were significantly superior to the CB plans. For the mean block structure contouring workload comparison, the LB plans (7·8 ± 0·6 minutes) were significantly better than the OB (9·3 ± 0·6 minutes) and CB plans (17·0 ± 1·6 minutes).

Regarding the plan quality score, the highest total score was shown in the CB plans (14 points) which provided the superiority of V_{5Gy}, integral dose and contralateral breast-sparing. On the other hand, the OB plans (4 points) provided the superiority of TT and block structure contouring workload. The OB and CB plans showed a trade-off between TT and normal tissue sparing. However, when focusing on the clinical practice issue in the low-dose spreading and TT, the LB plans (8 points) showed the balancing of plan efficiency by improving V_{5Gy}, integral dose, TT and block structure contouring workload with the highest score from all clinical practice concerning parameters.

Additionally, LB plans provided superior V_{5Gy} and equal integral dose compared with the OBDB, whereas TT and block structure contouring workload were slightly higher than the unblocked technique.

Even though some reports in modifying the HT treatment plan for limiting the low-dose volume spreading were published, but this study is the pioneer which concerned about the TT for implementation in clinical practice. Moreover, this study attempts to create a virtual block structure to reduce the volumes of normal tissue receiving low doses and minimise TT to reduce the impact of intrafraction motion and whole-body integral dose.[16] However, this study has limitation in small sample size. A study with larger

https://doi.org/10.1017/S1460396922000450 Published online by Cambridge University Press

sample size is the next plan to develop block structure technique which tailor to individual patient anatomy.

Conclusion

Regarding the plan quality score, the highest total score was shown in the CB plans which consumed the longest TT and block structure contouring workload. On the other hand, the OB plans provided the superiority of TT and block structure contouring workload but showed the inferiority of low-dose volume spreading. Therefore, the LB technique is considered to be the suitable technique for left-sided PMRT with RNI because of the balancing of plan efficiency by improving V_{5Gy}, integral dose, TT and block structure contouring workload with the highest score while maintaining the plan quality within the acceptable criteria as well.

Acknowledgements. The authors wish to thank staffs of the Division of Radiation Oncology, Faculty of Medicine, Chiang Mai University for supporting the data of this study.

Conflicts of Interest. No conflicts of interest.

References

1. Jones R T, Read P W, Shoushtari A N, Khandelwal S R, Sheng K. Class solution for post-mastectomy chest wall and regional nodal radiotherapy using tomotherapy. Int J Radiat Oncol Biol Phys 2010; 78 (3): 830.
2. Remick J, Amin N P. Postmastectomy breast cancer radiation therapy. In: StatPearls. Treasure Island, FL: StatPearls Publishing, 2021.
3. Nichols G P, Fontenot J D, Gibbons J P, Sanders M E. Evaluation of volumetric modulated arc therapy for postmastectomy treatment. Radiat Oncol 2014; 9: 66.
4. Chitapanarux I, Nobnop W, Tippanya D et al. Clinical outcomes and dosimetric study of hypofractionated helical tomotherapy in breast cancer patients. PLoS One 2019; 14 (1): e0211578.
5. Nobnop W, Phakoetsuk P, Chitapanarux I, Tippanya D, Khamchompoo D. Dosimetric comparison of TomoDirect, helical tomotherapy, and volumetric modulated arc therapy for postmastectomy treatment. J Appl Clin Med Phys 2020; 21 (9): 155–162.
6. Tang D, Liang Z, Guan F, Yang Z. Dosimetric and radiobiological comparison of five techniques for postmastectomy radiotherapy with simultaneous integrated boost. BioMed Res Int 2020; 2020: 9097352.
7. Ito M, Shimizu H, Aoyama T et al. Efficacy of virtual block objects in reducing the lung dose in helical tomotherapy planning for cervical oesophageal cancer: a planning study. Radiat Oncol 2018; 13 (1): 62.
8. Shiau A C, Hsieh C H, Tien H J et al. Left-sided whole breast irradiation with hybrid-IMRT and helical tomotherapy dosimetric comparison. BioMed Res Int 2014; 2014: 741326.
9. Davidson M T, Blake S J, Batchelar D L, Cheung P, Mah K. Assessing the role of volumetric modulated arc therapy (VMAT) relative to IMRT and helical tomotherapy in the management of localized, locally advanced, and post-operative prostate cancer. Int J Radiat Oncol Biol Phys 2011; 80 (5): 1550–1558.
10. Reynders T, Tournel K, De Coninck P et al. Dosimetric assessment of static and helical TomoTherapy in the clinical implementation of breast cancer treatments. Radiother Oncol 2009; 93 (1): 71–79.
11. Kraus K M, Kampfer S, Wilkens J J, Schüttrumpf L, Combs S E. Helical tomotherapy: comparison of Hi-ART and Radixact clinical patient treatments at the Technical University of Munich. Sci Rep 2020; 10 (1): 4928.
12. Yeh H P, Huang Y C, Wang L Y et al. Helical tomotherapy with a complete-directional-complete block technique effectively reduces cardiac and lung dose for left-sided breast cancer. Br J Radiol 2020; 93 (1108): 20190792.
13. International Commission on Radiation Units and Measurements. Report83: prescribing, recording, and reporting photon-beam intensity-modulated radiation therapy (IMRT). J ICRU 2010; 10 (1): 1–106.
14. Feuvret L, Noël G, Mazeron J J, Bey P. Conformity index: a review. Int J Radiat Oncol Biol Phys 2006; 64 (2): 333–342.
15. Ślosarek K, Osewski W, Grządziel A et al. Integral dose: comparison between four techniques for prostate radiotherapy. Rep Pract Oncol Radiother 2014; 20 (2): 99–103.
16. Sharma D S, Gupta T, Jalali R, Master Z, Phurailatpam R D, Sarin R. High-precision radiotherapy for craniospinal irradiation: evaluation of three-dimensional conformal radiotherapy, intensity-modulated radiation therapy and helical TomoTherapy. Br J Radiol 2009; 82 (984): 1000–1009.